Trends in Chemistry

CellPress REVIEWS

Focus on Perovskite Materials

Review

Excitons in 2D Organic–Inorganic Halide Perovskites

Catherine M. Mauck[1] and William A. Tisdale[1,*]

Layered perovskites are hybrid 2D materials, formed through the self-assembly of inorganic lead halide networks separated by organic ammonium cation layers. In these natural quantum-well structures, quantum and dielectric confinement lead to strongly bound excitonic states that depend sensitively on the material composition. In this article, we review current understanding of exciton photophysics in layered perovskites and highlight the many ways in which their excitonic properties can be tuned. In particular, we focus on the coupling of exciton dynamics to lattice motion and local distortions of the soft and deformable hybrid lattice. These effects lead to complex excited-state dynamics, presenting new opportunities for design of optoelectronic materials and exploration of fundamental photophysics in quantum confined systems.

Highlights

Two-dimensional layered perovskites (2DLPs) are solution-processed semiconductors that form natural quantum wells with high exciton binding energies.

Excitonic properties can be tuned in multiple ways, including: electronic bandgap, exciton binding energy, and exciton lifetime.

Exciton dynamics in 2DLPs are complex due to the hybrid organic–inorganic nature of the polarizable, relatively soft lattice.

Spectroscopic signatures indicate strong exciton–lattice interactions through the formation of polarons, which are electronic excitations dressed in the surrounding deformation of the polar lattice.

Exciton coupling to lattice motion in the form of local reorganization or optical and acoustic phonons is not yet fully understood.

Layered Perovskites: Self-Assembled 2D Optoelectronic Materials

Hybrid organic–inorganic lead halide layered perovskites are an exciting class of 2D materials that have sparked renewed interest for next-generation optoelectronic applications. This is in part due to the record power conversion efficiencies achieved by bulk perovskites, which outperform other solution-processed active layer materials by a wide margin [1,2]. Lead halide networks of $[PbX_6]^{2-}$ octahedra (Figure 1A) are templated into the $APbX_3$ perovskite structure (Figure 1B) by the incorporation of small central cations [A = methylammonium (MA), formamidinium (FA), cesium, and others]. The bandgap is entirely determined by the Pb and X orbitals and thus can be readily tuned by variation of the halide (X = chloride, bromide, iodide) [3,4]. Bulk perovskites are much more disordered than traditional high-purity silicon, yet possess surprisingly high defect tolerance as well as small **exciton binding energies (E_b)** (see Glossary) [5,6]. Furthermore, because perovskite composition is modular and prepared from solution, the dimensionality of the lead halide network is quite versatile and 0D, 1D, and 2D structures are easily accessed [7].

2D layered perovskites (2DLPs) consist of lead halide-networked sheets sandwiched between insulating organic cations (Figure 1C), which are bound coulombically to $[PbX_6]^{2-}$ as well as through ammonium-halogen hydrogen bonds. By changing the stoichiometry of the components and choosing organic cations (R) that are too large to fit in the cubic interstices, layered structures are formed with general chemical formulae R_2PbX_4. The hybrid structure leads to **quantum confinement** within the inorganic sheets, comprising a natural quantum-well (QW) structure (Figure 1D). The exciton confinement is enhanced by the presence of the organic lattice barrier that further confines the well dielectrically [8–10], leading to extremely high E_b on the order of several hundreds of meV [7]. In contrast to their 3D counterparts, these properties make 2DLPs excellent emitters and therefore well-suited for many photonics applications [11–13]. These include tunable, efficient lasers [14,15], light-emitting diodes (LEDs) [16,17], and photodetectors [18,19]. However, their strong absorption and superior environmental stability compared with 3D perovskites have also led to their incorporation into photovoltaic cells [20,21] and luminescent solar concentrators [22].

[1]Department of Chemical Engineering, Massachusetts Institute of Technology, 77 Massachusetts Avenue, Cambridge, MA 02139, United States

*Correspondence: tisdale@mit.edu (W.A. Tisdale).

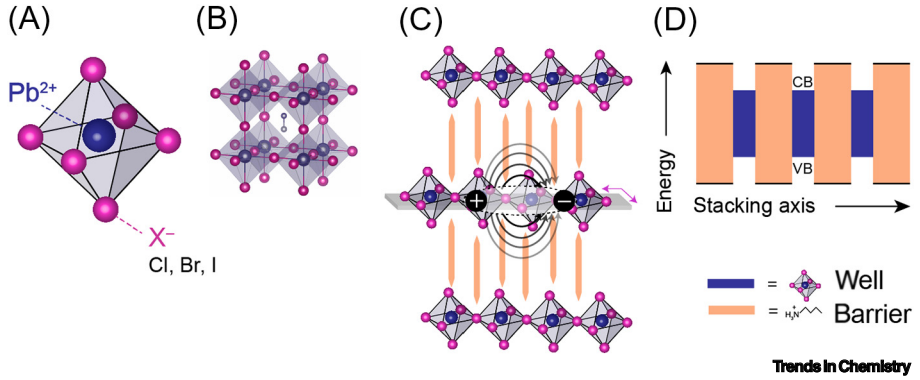

Figure 1. Structures of Lead Halide Perovskites Exhibit Dimensional Tunability and in Two Dimensions Are Characterized as Natural Quantum Well Systems. (A) The fundamental unit of the perovskite structure is the $[PbX_6]^{2-}$ octahedron, which can assemble into (B) the 3D cubic perovskite structure, shown here for methylammonium (MA) lead iodide, where X = Cl^-, Br^-, I^- and MA occupies the interstitial central cation site. (C) With appropriate stoichiometric preparation, 2D layered perovskite (2DLP) structures self-assemble into (D) natural multiple quantum well structures, where high dielectric lead iodide stacks experience both quantum confinement within the 2D plane as well as dielectric confinement due to interlayer low dielectric organic cations [32].

Structural Diversity in Hybrid Materials

Many diverse layered perovskite structures have been reported (Figure 2), due to both the tunability of the inorganic lattice composition as well as the relatively unrestricted parameter space of the organic cation [13]. Like their bulk counterparts, the **bandgap energy (E_g)** of 2DLPs is determined by overlap of the Pb/X bonds, and can range from UV to near infrared, depending on the halide anion [23] and the thickness of the inorganic sheet (*n*) [24]. The organic layer does not affect the electronic properties directly; instead, the packing of the organic layer in concert with noncovalent R-PbX interactions will template formation of the inorganic network and with it the inorganic orbital overlap (Figure 2C). Although the inorganic lattice is most commonly formed as a (100)-oriented flat sheet of corner-sharing $[PbX_6]^{2-}$ octahedral [13], their connectivity can vary, leading to more exotic structures such as the (110) zig-zag [25] or corrugated structures [26] (Figure 2C) and edge- and face-sharing octahedra networks (Figure 3A, Key Figure) [27]. The organic layer determines other properties of the hybrid 2DLP as well, such as its hydrophobicity and stability [21,28,29], structural rigidity [20,30], sheet-to-sheet distance [31–33], and the dielectric screening experienced by charge carriers confined within the inorganic layer [34–36].

Early work focused primarily on $n = 1$ layered perovskites, in which the alternating stacks of organic cations surround atomically thin inorganic sheets [3,9,37–40]. However, recent work has extensively centered on variable well thickness in layered structures with $n > 1$, in particular the Ruddlesden–Popper-phase perovskites (RPPs, Figure 2A) [24]. Instead of a single layer of lead halide octahedra, this class of layered perovskites contains the classic ABX_3 perovskite structure (with central cation, A) within each inorganic sheet, layers of which are spaced by the larger organic cations R. The well thickness *n* and E_g is stoichiometrically determined by the ratio of R:A (Figure 3C), with formula $R_2A_{n-1}B_nX_{3n+1}$. These materials are sometimes called 'quasi-2D', as they possess both the layered stacking of 2DLPs, as well as the polarizable central cation-templated cubic structure of 3D perovskites. Consequently, RPP perovskites have properties of both types of structures and have been studied extensively for photovoltaic applications [1,13,41,42]. Several other classes of 2D perovskite phases have been the focus of recent work, particularly the Dion–Jacobson [43] and alternating-cation-interlayer [44] types of formula $A'A_{n-1}B_nX_{3n+1}$ and $A'A_nB_nX_{3n+1}$, respectively (Figure 2B). These phases are distinguished from RPP structures by their eclipsed inorganic layer stacking and smaller interlayer spacing, leading

Glossary

Bandgap energy (E_g): in a semiconductor, the energy difference between an electron in the highest energy level of the valence band and the lowest energy level of the conduction band; also referred to as the quasiparticle gap, E_g.

Bandgap renormalization: a change in the electronic bandgap energy of a semiconductor following photoexcitation. In 2D semiconductors, a high density of photogenerated carriers will screen repulsive Coulomb interactions between charge carriers of the same sign, leading to a net decrease in the electronic bandgap energy.

Exciton binding energy (E_b): minimum energy required to ionize a bound electron–hole pair from its lowest energy eigenstate into uncorrelated free charge carrier states. The exciton binding energy, E_b, is usually given a positive sign for net attractive interaction.

Exciton Bohr radius: a measure of the maximum probability density of the Coulomb interaction between an electron and hole in an exciton. This value can serve as a proxy for the size of the exciton in a given material.

Exciton fine structure: the splitting of excitonic states into multiple sublevels, characterized by their energetic spacing, degeneracy, oscillator strength, and spin characteristics.

Frenkel excitons/Wannier–Mott excitons: the extent to which an exciton is delocalized will determine whether it is of Frenkel or Wannier character, based on how the excitonic electron–hole
Coulomb interaction is screened by its surrounding dielectric environment. In a high-dielectric material, the attractive Coulomb interaction is well-screened and the exciton is Wannier-like. In this case the exciton has a large Bohr radius and delocalizes over many molecules or unit cells. However, in a low-dielectric material, the electron and hole are tightly bound because the Coulomb interaction is poorly screened and the exciton is Frenkel-like. The exciton Bohr radius is small and the exciton is highly localized to a single molecule or unit cell.

Photoluminescence quantum yield (PLQY): a metric of the fluorescence efficiency of a material, equivalent to the number of photons emitted divided by the number of photons absorbed.

Polaron: a charge carrier that has created its own potential well via

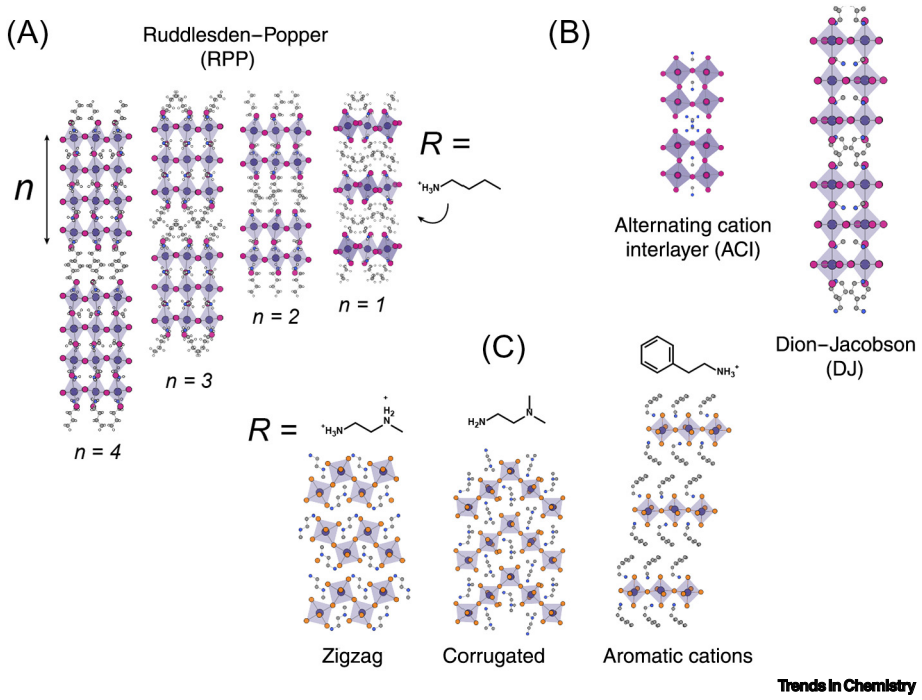

Figure 2. Structural Diversity of Lead Halide Perovskites. (A) Ruddlesden–Popper phase (RPP) perovskites [24] with well thicknesses n = 1–4, where n represents the number of lead octahedra layer stacks. When $n > 1$, the inorganic sublattice comprises the full ABX_3 perovskite structure containing small central cations, in addition to larger the organic interlayer cation. (B) Other variable well thickness 2D perovskite phases are depicted, where the inorganic–inorganic layer spacing is much smaller than in the RPP structures, which subsequently lowers the bandgap energy. (C) Organic interlayer cations indirectly affect the electronic bandgap in 2D layered perovskites (2DLPs) through templating of the lead halide network via complex intermolecular interactions. More exotic 2DLP structures such as zigzag [α-(DMEN)$PbBr_4$] [100], corrugated [(*N*-MEDA)$_2PbBr_4$] 2DLP structures [26] are possible, in addition to the incorporation of a variety of different functional organic cations, with phenethylammonium lead bromide shown here [28].

to lower bandgap energies due to weak interactions between adjacent inorganic layers [13]. Here, we focus on the family of RPP perovskites, which have been the most widely studied in terms of exciton dynamics, but the conclusions drawn from their consideration are applicable to the wide diversity of low dimensional perovskite structures.

Modular Design for Tunable Electronic Properties

2DLP materials have been studied for several decades, but in the context of recent intense interest in lead halide perovskites, the complex nature of their excitonic properties is only now beginning to be revealed. Befitting their hybrid nature, they share similarities with a diverse set of materials: they possess excitonic confinement with similarities to monolayer transition-metal dichalcogenides, disorder and self-assembly similar to organic semiconductors, and band structures that resemble traditional inorganic QWs. What is perhaps most exciting about 2DLPs, in contrast to these other semiconductor materials, is their virtually infinite tunability as demonstrated in Figure 3. With optical absorption that can be varied through halogen alloying [45] and the dielectric environment and lattice order/disorder indirectly affected by choice of the organic cation (Figure 3D) [13,46], such precise and accessible synthetic control is unprecedented.

Variable E_b

Tuning of the E_b is beneficial for optoelectronic applications, for example, in solar cells in which 2DLPs are used as high-energy absorbers and protective moisture barriers [13,21,29].

structural deformation of the surrounding lattice. A **large polaron** extends over multiple unit cells of the structural lattice and behaves like a free charge carrier, but with a heavier effective mass and reduced scattering. A **small polaron** is localized to a single structural site and moves by thermally activated site-to-site hopping.

Quantum confinement: in a material whose dimensions are smaller than its exciton Bohr radius, an excitation will be confined in space, causing its energy levels to be quantized (i.e., discrete).

Rashba splitting parameter: a material constant that determines the magnitude by which spin-polarized bands are offset from the zone center (k = 0) in noncentrosymmetric compounds exhibiting strong spin-orbit coupling.

Self-trapped exciton (STE): similar to a small polaron, a self-trapped exciton is an electron–hole pair that has become localized to a single lattice site through displacement of nearby ions from their equilibrium positions.

Spin-orbit coupling: interaction between an electron's spin and its orbital angular momentum that breaks state degeneracy. For heavy atoms such as lead, this relativistic effect is significant.

Key Figure

Modular Tunable Design Enables Targeting of Desired Properties

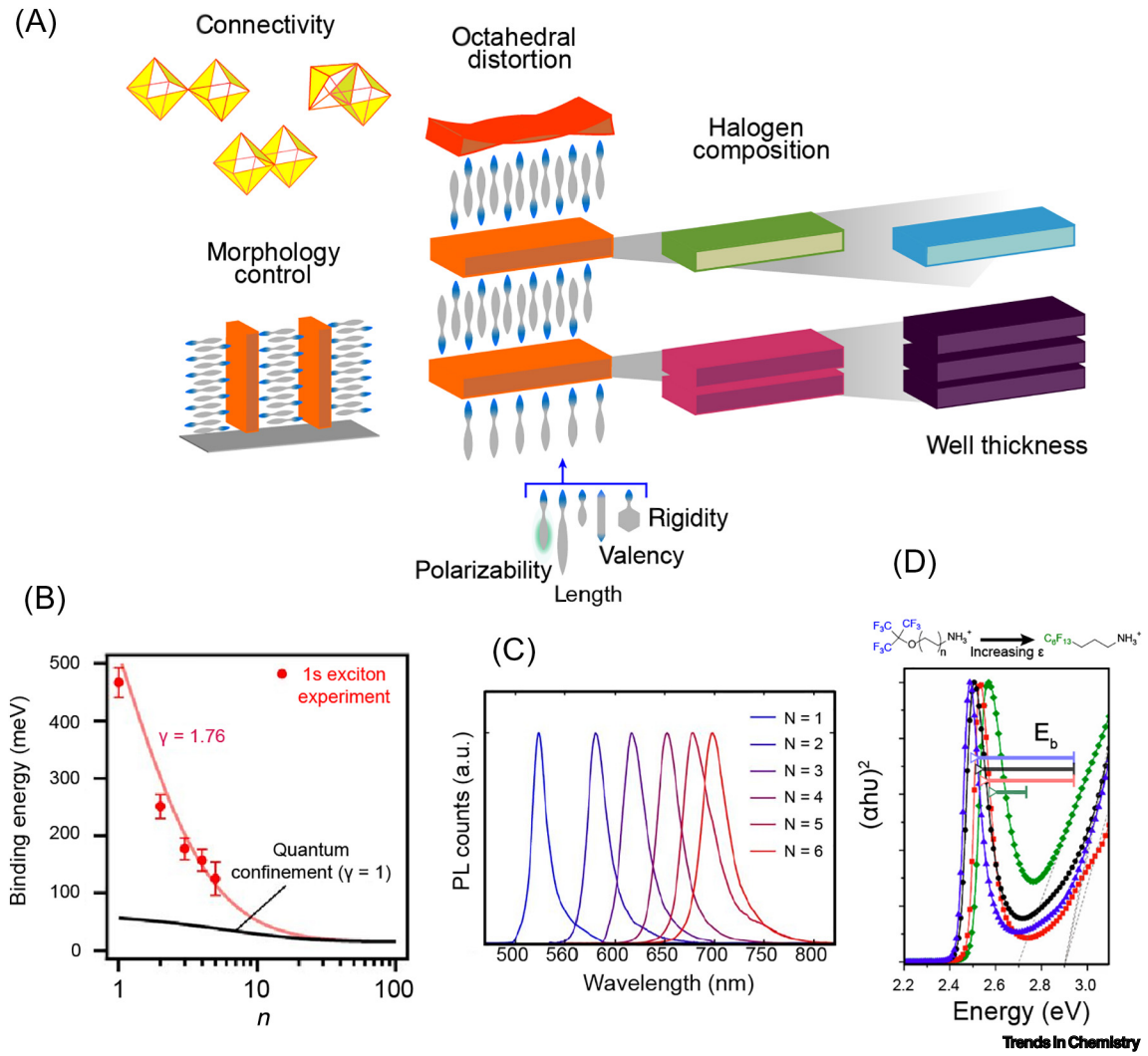

Figure 3. (A) 2D layered perovskite (2DLP) structures are modular and enable compositional control over optoelectronic properties. Tunable parameters include octahedra connectivity motifs (corner sharing, edge sharing, or face sharing), degree of octahedral distortion within the lead halide plane, film growth orientation and morphology, bandgap tuning through halide alloying, the organic cation length, valency, rigidity or aromaticity, and (C) well thickness *n* for Ruddlesden–Popper perovskites, and (B) tuning of exciton binding energy as a function of *n*, as well as (D) the polarizability of the organic cation such as increasing fluorous content of organic ligand on the absorption. Panels (B,C) reproduced with permission from [47] and [67]. Panel (D) adapted with permission from [51]. Abbreviations: PL, Photoluminescence.

One manner in which E_b may be controlled is through the well thickness and stoichiometry of RPP perovskites (Figure 3B), as in a traditional QW, although this also lowers the E_g [24,42]. Mohite and colleagues have outlined a scaling law for E_b as a function of well thickness *n*, that more accurately accounts for dielectric confinement effects;

their model predicts that excitons are stable at room temperature below well thicknesses $n = 20$ [47].

Others have targeted postsynthetic modification, such as in the work by Karunadasa and colleagues, demonstrating tunable **exciton binding energy (E_b)** from reversible iodine gas chemisorption in an $n = 1$ 2DLP [48,49]. They pursued this strategy further by incorporating iodohexylammonium cations to directly enhance the organic interlayer polarizability, thereby reducing E_b from >300 to ~200 meV [50]. By subsequently exposing the 2DLP film to iodine gas, E_b was further decreased to 180 meV (Figure 3D). Grancini and colleagues also studied several different fluorous organic cations to tune E_b in lead iodide 2DLPs (Figure 3D), which also showed improved stability due to their enhanced hydrophobicity [51].

Octahedral Distortion and Broadband Emission

Certain 2DLPs have strong, broad emission from below-bandgap states (Figure 4), spanning the 500–900 nm spectral region and presenting intriguing possibilities as white light emitters in solid-state lighting [52,53]. The connection between structural distortion and the relative intensity of this white light emission has been investigated by exploiting the diverse tunability of 2DLP structures [25,31,52,53]. Petrozza and colleagues found that 2DLPs with inorganic lattice geometries that deviate more from an ideal octahedron correlate with broad, low energy emission, by using the mean octahedral elongation and octahedral angle variance as measures of distortion in 13 published 2DLP crystal structures [53]. Similarly, Karunadasa and colleagues analyzed eight lead bromide perovskites with regard to more than 50 crystallographic parameters, and determined that the metal–(μ-halide)–metal angle, separated

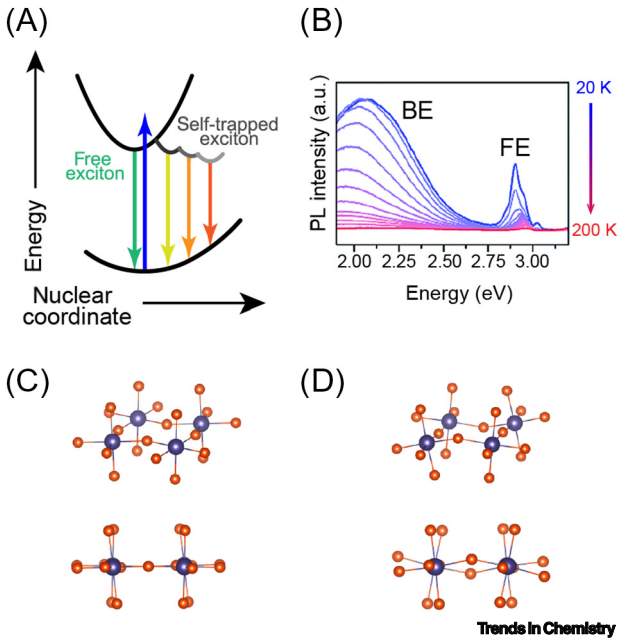

Figure 4. Octahedral Distortion, Exciton Self-Trapping, and White Light Emission in 2D Layered Perovskites (2DLPs). Upon light absorption in 2DLPs, energy can be emitted at the 'free exciton' (FE) energy, or as lower energy, broadband emission (BE) due to lattice reorganization in the presence of the exciton, assigned to exciton self-trapping. Energy diagram (A) and representative photoluminescence (PL) spectra (B) as a function of temperature show that I_{FE}:I_{BE} depends on the energy available to escape shallow traps. (C) In-plane octahedral distortion is shown in comparison with (D) out-of-plane octahedral distortion which tends to enhance white light emission in 2DLPs. Structure and spectra adapted with permission from [52].

into its in plane and out of plane components, had the strongest correlation with broadband emission (Figure 4C,D) [52].

Broadband emission in 2DLPs is understood to be an intrinsic phenomenon related to the deformability of the lattice, rather than material defects. The presence of the exciton itself causes a local lattice reconfiguration, forming a low-energy self-trapped state that is associated with white light emission [54]. These **self-trapped excitons (STEs)** are conceptually analogous to **small polarons** [53,55], wherein a charge carrier distorts the surrounding structural lattice, creating a local potential well in which the charge carrier is self-trapped [56]. Self-trapped states are in thermal equilibrium with the free-exciton states, existing as a distribution of locally distorted states with measured activation energies below kT (Figure 4A) that leads to broadband emission with large Stokes shifts [31]. These polaron-excitons have been modeled with density functional theory (DFT) calculations as self-localized carriers analogous to alkali halide crystals [54], to obtain formation energies of possible transient defects originating from bond shortening within the lead halide. Calculations indicate that negatively charged iodide centers are the most likely to form [57]. Experiments as well as molecular cluster computation indicate that both positive and negative trap states are possible [54,55] in the exciton case where a trapped hole will cause distortion that leads to an electron trapping site, and vice versa [55].

In transient absorption (TA) experiments, STE signatures appear on a wavelength-dependent sub-picosecond or picosecond timescale, and thus are distinguished from nontransient trap sites due to material defects [31]. STEs typically have longer lifetimes than free exciton emission; in (EDBE)PbX_4 compounds the free exciton emission has a ~ 10 ps lifetime, in contrast to the white light emission with lifetimes of roughly 1–3 ns [54]. Similarly, in time-resolved photoluminescence (PL) measurements on a 2D cyclohexylammonium lead bromide, the white light emission features decayed biexponentially with time constants on the order of several nanoseconds, and up to microseconds at low temperature [54,58].

Controlling Morphology

Another important parameter is the morphology and conductivity of 2DLPs, particularly in a photovoltaic active layer where sunlight is absorbed, and excitons separated into charge carriers. Because 2DLPs typically grow parallel to the substrate, the conductive, inorganic layers are insulated from the contacts by the organic interlayers. Recent advances have achieved perpendicular growth in RPP films to enhance carrier injection into charge collecting layers, notably through the 'hot casting' method pioneered by Kanatzidis and colleagues [41,59]. Choi and colleagues succeeded in assembling vertically oriented $BA_2MA_3Pb_4I_{13}$ films (i.e., $n = 4$) by using dimethylacetamide as the spincoating precursor solvent, achieving high power conversion efficiency (PCE) for a 2DLP photovoltaic device [60]. For LED applications, Mohite, Kanatzidis, and coworkers have combined the hot-casting method with synthesis of phase-pure RPP perovskites of $n > 2$ to engineer vertically oriented 2DLP LEDs of high color purity and improved operational stability [61]. Device efficiency of photovoltaics containing only 2DLPs as the active layer has been generally poor due to inefficient charge separation [28,59], but recent studies have shown that a combination of 2DLPs with 3D perovskites can maintain high PCE for twice as long as 3D perovskite active layers alone [29,42]. Techniques targeting film morphology and orientation should continue to be pursued and are expected to yield further advances in optoelectronic device optimization.

Excitons in a Hybrid Crystal Lattice

In contrast to conventional inorganic semiconductors, the structural lattice of lead halide perovskites is soft and highly polar [62]. Additionally, the combination of organic and inorganic components leads to exciton dynamics that resemble both inorganic 2D QWs and organic

semiconductors. TA spectroscopy, which measures the change in transmission as a function of time after photoexcitation, has been used to study $n = 1$ perovskite films, finding that spectra can be characterized by a sub-picosecond blue shift of the 1*s* exciton resonance (Figure 5E) [63]. This dynamic blue-shift arises from complex many-body interactions in 2D semiconductors. On one hand, screening of repulsive Coulomb interactions between charge carriers of the same sign leads to a reduction in the bandgap energy. Alone, this **bandgap renormalization** would cause a red-shift in the excitonic transition energy [64,65]. However, the red-shift is offset by an

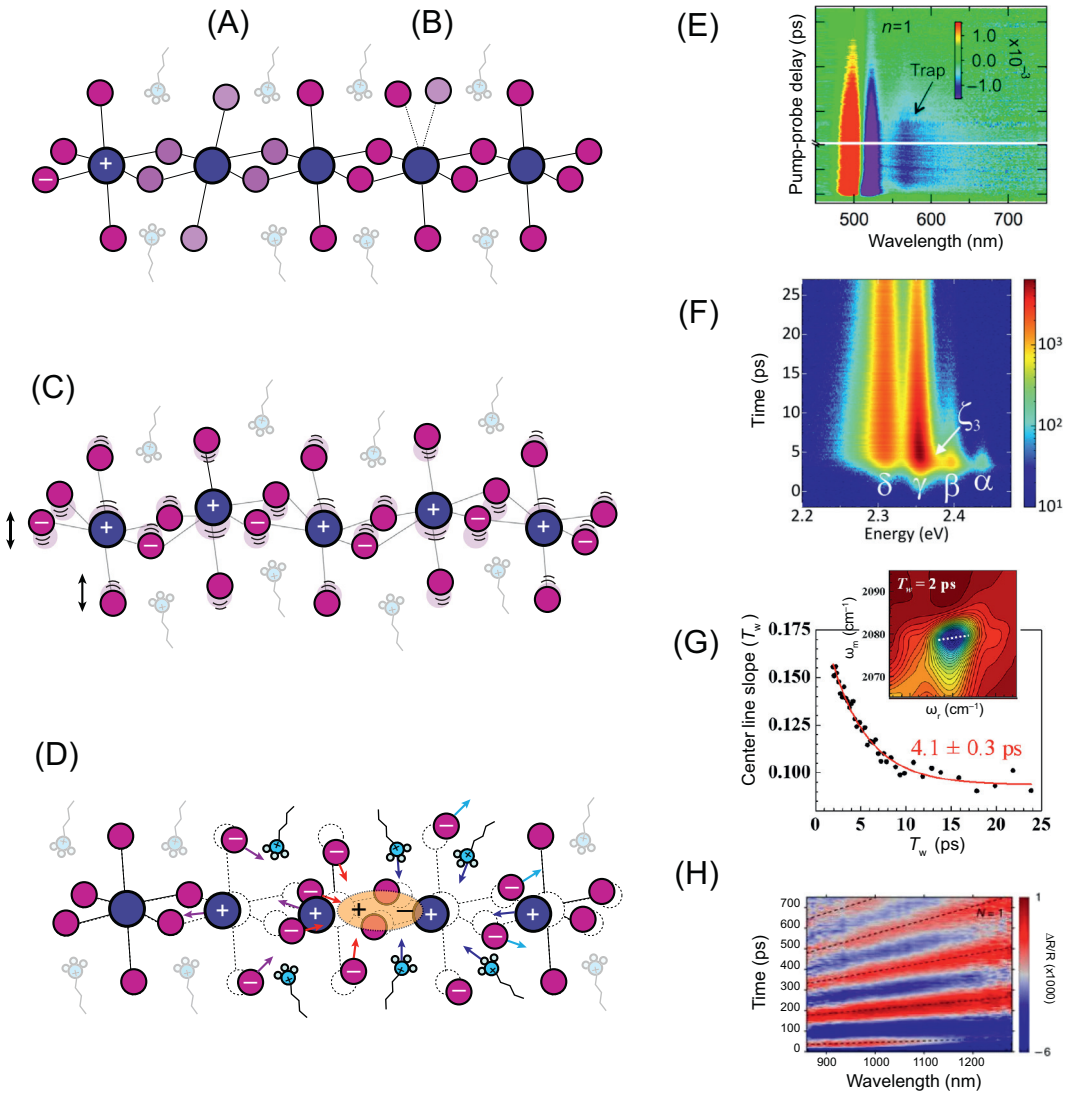

Figure 5. Lattice Motion and Configurations Contributing to Exciton Dynamics in 2D Layered Perovskites (2DLPs). (A) Local variations in lattice configuration can occur, as well as (B) defect sites such as I_i^- interstitials, that represent static disorder. Panel (C) shows collective lattice motion across more than one unit cell, corresponding to a phonon. The presence of charge carriers or excitons within the inorganic network can cause local reconfiguration of the lattice in response, leading to a polaron, illustrated in (D). (E) Transient absorption spectra for an $n = 1$ 2DLP are shown, characterized by an ultrafast shift due to bandgap renormalization and later population of shallow trap states. (F) Phonon sidebands appear in the transient photoluminescence spectra in a 2DLP. (G) Thermal disorder is probed by the decay of 2D infrared spectroscopy (2DIR) features. (H) Evidence for coherent longitudinal acoustic phonons is shown in transient reflectance measurements, reproduced with permission from [67]. Panel (E) reprinted with permission from [63], panel (F) reprinted with permission from [69], and panel (G) adapted with permission from [72].

even larger reduction in the E_b due to screening of the electron–hole Coulomb interaction by photogenerated charge carriers, leading to a net blue-shift of the exciton resonance. Additionally, many studies have pointed to the important role of electron-phonon coupling in the excited-state dynamics of 2DLPs [20,46,66–68]. As shown schematically in Figure 5, factors affecting excited-state dynamics include thermal disorder, static defects and heterogeneity, scattering of carriers by collective vibrational lattice motions in the form of phonons, and polaron-like lattice reconfigurations [53].

Exciton–Phonon Coupling

Coupling between excitons and phonons is relatively strong in 2DLPs [20,46]. In polar crystals, including perovskites, carrier scattering is understood to be dominated by coupling to longitudinal optical (LO) phonons. Several studies have observed strong excited-state coupling to a 12–14 meV lattice mode in 2DLPs [66,69], close in energy to that of the PbI_2 LO phonon (13.7 meV) [70]. Five other low energy phonons from 8–17 meV in various 2DLP structures have also been resolved with ultrafast (<20 fs pulse) TA spectroscopy, such as in the impulsive Raman signatures of the 2DLP excited state [72] and in 2D coherent excitation spectra [66,71]. However, the vibrational spectra that result from these experiments indicate that the exciton couples to a multiplicity of contributing modes, with certain modes affected by the length of the organic cation [66,68,71].

In addition to optical phonons, coherent longitudinal acoustic phonons have been observed in n = 1–6 2DLPs by transient reflectance measurements (Figure 5H), induced by hot exciton generation and probed below the bandgap [67]. The authors found that cross-plane group velocities in 2DLPs are consistently slower than in bulk $MAPbI_3$, which they attribute to an impedance mismatch at the organic–inorganic interface that suppresses phonon transport. These findings have important implications for thermal dissipation in 2DLP-based devices; for example, they report that lengthening the organic spacer should lead to faster phonon propagation.

Sargent and colleagues have also undertaken detailed computation and scattering experiments to determine that the crystal rigidity is a crucial parameter for obtaining high **photoluminescence quantum yield (PLQY)** in 2DLPs, as lowered organic lattice motion reduces nonradiative processes [20]. That study and other notable work by Yang and colleagues on atomically thin $(C_4H_9NH_3)_2PbX_4$ sheets [23] has demonstrated that 2DLPs are excellent candidates to meet the challenge of high-efficiency, high-purity blue emission for LEDs [20].

Contributions from Dynamic Disorder

The origins of dynamic changes in local lattice configuration are complex in these deformable, hybrid materials, and not adequately described by exciton–phonon coupling alone. The timescale of dynamic disorder was measured directly through 2D infrared (2DIR) spectroscopy in $(MA)_2PbI_2(SCN)_2$ using the isotopically diluted ^{12}CN stretch to report on the local environment in response to excitation, where the coupling interaction of adjacent CN vibrations decayed with $\tau \sim 4$ ps (Figure 5G) [72]. The authors argue that it is thermal fluctuations sampling many different local lattice configuration minima within an inhomogeneously broadened distribution that causes this dynamic disorder. They emphasize that these configurations are distinct from coupling to collective lattice motions (i.e., phonons). Silva and colleagues have also used 2D electronic spectroscopy to explore the interplay between phonon coupling and local lattice fluctuation in 2DLPs and argued that on the ultrafast timescale spectral diffusion dominates [73].

Exciton-Polarons

In 3D perovskites, free charge carriers are thought to exist as **large polarons** [62,74,75]. Large polarons are charge carriers dressed in the deformation of the surrounding polar lattice. In

contrast to small polarons, large polarons extend over multiple unit cells and behave much like free charge carriers. However, large polarons are characterized by a heavy effective mass and screening of the charge carrier by the lattice polarization, resulting in reduced scattering with other charge carriers, defects, and polar optical phonons [56,76].

In 2DLPs, free excitons most likely exist as large exciton-polarons, or bound excitonic resonances that are partially solvated by polarization of the surrounding ionic lattice extending over multiple unit cells. In contrast to the localized STEs described earlier, these large exciton-polarons should be highly mobile and difficult to distinguish from nonpolaronic free excitons. Careful spectroscopic investigation will be required to accurately characterize their properties.

Hybrid Exciton Interactions with Polarons

The hybrid nature of excitons in 2DLPs was a central focus of early work [77,78]. The physical size and binding energy of an exciton depends on how effectively the surrounding environment screens the electron–hole Coulomb interaction. In a high-dielectric material such as silicon, the Coulomb interaction will be well screened and the exciton is described as a **Wannier–Mott exciton**, which characteristically has a large effective radius but low binding energy. However, in low-dielectric semiconductors such as organic crystals, the dielectric environment cannot effectively screen the electron–hole interaction; instead, the exciton is tightly bound, with a small radius and high binding energy. This is the **Frenkel exciton** picture, typically associated with molecular systems. 2DLPs represent an interesting case because they are hybrid materials that combine both inorganic semiconductors (i.e., PbI_2) and molecular crystals (i.e., organic cations $R_2NH_3^+$). Consequently, excitons in 2DLPs are hybrid as well, and depending on the model used to treat the exciton in these materials, vastly different **exciton Bohr radii** have been derived, from 0.1 to 2 nm [9,46,79,80].

Silva, Srimath, and colleagues introduced both Frenkel and Wannier formalisms to their analysis of temperature-dependent absorption, PL, and 2D TA spectra of $(PEA)_2PbI_4$ [71]. The authors observed oscillations of off-diagonal features in the 2D TA spectra at the same frequency as the spacing between sidebands in the ground-state excitonic absorption spectrum (~34 meV). They note that the 34 meV spacing of the sidebands does not correspond to a known vibrational energy, but is within the range of the calculated polaron energy. The authors propose that it is phonon-driven lattice distortions (polarons) that are responsible for the observed exciton absorption fine structure and that these features represent distinct excitonic states with renormalized binding energies, rather than phonon replicas. Additionally, because the excitons in 2DLPs experience both Frenkel-like localization along the stacking axis but Wannier-like delocalization within the 2D inorganic plane, scattering with an LO phonon mode ~17 meV is also significant, and is the dominant mode causing PL linewidth broadening. This study highlights the importance of considering the complex nature of exciton–phonon coupling in 2DLPs.

Heavy Atom Effects

Rashba splitting, in which strong **spin-orbit coupling** in the absence of inversion symmetry breaks the spin degeneracy of bands, is predicted to be particularly strong in 2DLPs (Figure 6) [81,82]. For example, the **exciton fine structure** in alkylammonium lead iodide 2DLPs shifts with increasing applied magnetic field [80]. This effect has been extensively investigated in 3D perovskites [81] and in fact should be more pronounced in lower dimensions [82–84], in particular for the heavy atom-containing lead iodide perovskites. But this phenomenon should occur statically in noncentrosymmetric structures only, as a recent theoretical and experimental paper establishes is the case for RPP perovskites of $n = 2$ but not for odd-numbered n [85]. Only by applying a strong external electric field were the authors able to observe Rashba splitting in an $n = 1$ perovskite. Another recent study by Van de Walle and colleagues concludes that Rashba

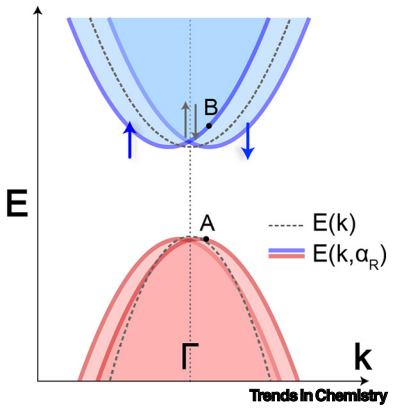

Figure 6. Rashba Effects. Electron dispersion diagram for Rashba splitting, which can occur in noncentrosymmetric structures when there is strong spin-orbit coupling, and breaks band degeneracy [dotted parabolas, E(k)] and results in two spin-polarized bands [$E(k,\alpha_R)$] where α_R is the Rashba splitting parameter.

effects actually shift the conduction and valence bands by the same amount, such that the direct band transition is preserved [86]. However, a very large **Rashba splitting parameter** was also reported in $n = 1$ perovskite $(PEA)_2PbI_4$, via electroabsorption measurements [84]. Given the strong dynamic disorder, local symmetry breaking in the presence of strong spin orbit coupling inevitably occurs. Recent molecular dynamics simulations in 3D $CsPbBr_3$ have found exactly that [87], which suggests that Rashba splitting should not be disregarded in 2DLPs, but Rashba effects even in bulk 3D perovskites are still debated.

The implications of spin have been infrequently invoked in discussions of 2DLP excited-state dynamics, but should be considered in future research. Indeed, in certain 2DLP structures, lower energy states have been assigned to triplet excitons instead of STEs, with lifetimes reaching 180 ns [77,88,89].

Exciton Fine Structure

At low temperature, excitonic absorption and emission features in 2DLPs separate into discrete peaks that are closely spaced in energy [68,69,71,78–80,90]. The origin of this exciton fine structure is the subject of some debate in the literature. For example, Kagan and colleagues [69] observed multiple peaks separated by a 40–46 meV spacing in the low temperature PL and absorption spectra of $(PEA)_2PbI_4$. Based on DFT calculations, they assigned these features to phonon replicas arising from coupling of the excitonic transition to a vibrational mode associated with organic cation motion. Interestingly, a similar spacing of ~35 meV was reported by Silva, Srimath, and colleagues in the low-temperature absorption spectrum of $(PEA)_2PbI_4$, but is attributed to distinct excitonic states that are coupled through polaronic effects [71]. Further work by this group has recently resolved vibrational coherences associated with the exciton [68]. Finally, Vardeny and colleagues observed a distinct peak at ~40 meV in the room-temperature electroabsorption spectrum of $(PEA)_2PbI_4$ and attributed it to Rashba splitting [84]. We note that the similarity in energy of the spectral features identified in each of these studies may indicate that these authors are observing the same phenomenon, although differing in their interpretation. Clear assignment of these spectral features is undoubtedly a focus of future work for this field.

Preventing Nonradiative Recombination through Energy Funneling

Previous perovskite-based LEDs have had poor electroluminescence at room temperature [91]. However, recent work on RPPs with mixed well thickness has lead external quantum efficiencies (EQE) >11% for emission at ~700 nm [16,17]. The improved radiative recombination efficiency is attributed to an energy cascade pathway available in RPP 2DLPs, in which grains of different n values funnel excitation from high- to low-energy states; in other words, in films of mixed-n

phases, carriers transfer from low-*n* to high-*n* grains, concentrating and finally recombining in the lowest bandgap phases. Both energy transfer [92] and electron transfer [93,94] are present in these mixed-*n* films, with the dominant funneling mechanism still under debate. In mixed RPP films, because E_b decreases as well thickness *n* increases, certain layers will have a higher ratio of excitons than charges and vice versa [95].

Energy funneling is further complicated by defect-assisted recombination [92]. So-called layer edge states were identified in exfoliated and few-layer $(BA)_2(MA)_{n-1}Pb_nI_{3n+1}$ crystals of $n > 2$ as free carrier traps, by spatially and temporally resolved PL [96]. Interestingly, an intergrain charge transfer state dependent on the organic cation concentration has also been invoked in $(PEA)_2PbI_4$ [97]. Intergrain interactions will be important factors in 2DLP device optimization.

Tuning Electronic Properties through Precise Molecular Control

In addition to film optimization, we emphasize that the precise, molecular-level structural tunability of 2DLPs is unique and should be fully exploited towards the understanding of the complex carrier dynamics in these hybrid materials. Already such synthetically targeted strategies have resulted in interesting results; for example, Stupp and colleagues have explored the effect of various planar organic cations on the out-of-plane conductivity and electronic properties of lead iodide layered perovskites [35]. They found that energy level alignment between the inorganic and organic lattice, as well as π–π interactions between adjacent organic interlayers, enhance the out-of-plane conductivity and improve the efficiency of 2DLP-based solar cells. In 2009, Galmiche and colleagues prepared a group of lead bromide and lead iodide 2DLPs with organic ammonium cations ranging from highly sterically hindered adamantane derivatives and flexible cyclohexyl rings to conjugated, rigid phenyl rings [98]. The resulting films showed that π–π interactions caused more ordered, crystalline films, and that the more flexible organic cations could stabilize broad, below-bandgap emission.

Galmiche and colleagues also studied the effect of alkyl chain spacer length between the ammonium and the organic moiety on the PL efficiency [98]. As others have found, the optimal spacer length for PLQY optimization varies based on the structure of the organic moiety. In some cases, lengthening the alkyl chain spacer can cause significant changes to the inorganic lattice, such as in work by Kamminga and colleagues where going from PEA to phenylbutylammonium cations causes lead iodide octahedra to form more face-sharing connections, leading to crystals with 1D quantum confinement instead of 2D [99]. A study from Mitzi and coworkers also centered on 2DLPs with structurally varied organic ammonium cations, by varying the alkyl spacer length in phenyl and naphthyl cations, and showing that certain octahedral planar distortions accommodate white light emission more readily [30].

Concluding Remarks

As these studies demonstrate, a major challenge for structurally targeted design of 2DLPs is that systematic molecular modifications have complex effects on lead halide octahedral geometries. The link between structure and optoelectronic properties is not direct, which explains the absence of comprehensive design rules for a desired optoelectronic property, despite numerous studies on a variety of structures. A change as simple as lengthening the alkylammonium cation by just two carbons can dramatically alter exciton–phonon coupling in 2DLPs [66], and such a simple structural perturbation is further complicated by the widely variable phase transition temperatures and symmetries as alkylammonium cation length increases from 4 carbons to 16 [32,33].

Outstanding Questions

What is the origin of the exciton fine structure: exciton–phonon coupling, Rashba splitting, or distinct excitonic states with renormalized binding energies?

To what extent does polaron formation renormalize the exciton energy, and how do polaronic effects influence exciton dynamics?

Are there design rules for intentional modification of 2DLP structure, degree of lead halide distortion, and connectivity through choice of organic cation?

Are there opportunities for the organic cation to function as more than a dielectric spacer?

This complicated picture emerges from the diversity of intermolecular interactions due to the inherent hybridicity of these 2D materials. Ionic interactions govern Pb-I octahedral assembly, but are also affected by inorganic–organic interactions between the sublattices in which the alkylammonium group forms halogen–hydrogen bonds; and the ammonium group in turn is covalently bound to the organic moiety, subject to van der Waals, π–π, and hydrophobic/hydrophilic interactions, as well as order/disorder transitions specific to the organic structure. Structural perturbations to the organic layer in which the inorganic layer is relatively unchanged represent a promising method to disentangle these contributions and will be necessary to enable strategic materials design in 2DLPs. Already, postsynthetic modifications such as those pursued by Karunadasa and others, with an emphasis on exciton self-trapping and white light emission, have been powerful for studying their effect on 2DLP electronic properties in a more controlled manner [25,34,48–50,52,100]. Strategies that tune E_b with precision will be important for photovoltaic applications, so that 3D perovskite solar cells with high efficiency but low environmental stability can be combined with the enhanced moisture stability of 2DLPs without sacrificing efficient carrier dissociation.

Additionally, the totality of carrier–lattice interactions in the deformable, flexible ionic crystal of 2DLPs must be considered in their totality, including Rashba effects [84], thermal disorder [72], optical and acoustic phonons [46,67], and polaron-induced transient disorder [55,71] With E_bs that far surpass kT at room temperature, these materials are promising emitters; yet due to their strong exciton–lattice coupling, they still suffer from low PLQY under ambient conditions because nonradiative pathways dominate. It will be important for device optimization to continue to explore how nonradiative recombination can be inhibited in these hybrid materials. Ultimately, much fundamental work remains to elucidate structure–function relationships and the mechanisms underlying exciton dynamics in 2DLPs (see Outstanding Questions), as their interesting optoelectronic properties continue to be explored and discovered. In addition to their interest for light emitting and light harvesting applications, these materials exhibit hyperbolic dispersion and extreme anisotropy [101], as well as room-temperature stable biexcitons [73], opening the way for further study of interesting and unusual physics.

References

1. Rong, Y. *et al.* (2018) Challenges for commercializing perovskite solar cells. *Science* 361, eaat8235
2. Green, M.A. *et al.* (2014) The emergence of perovskite solar cells. *Nat. Photonics* 8, 506–514
3. Mitzi, D.B. (2001) Templating and structural engineering in organic-inorganic perovskites. *J. Chem. Soc. Dalton Trans.* 1, 1–12
4. Herz, L.M. (2016) Charge-carrier dynamics in organic-inorganic metal halide perovskites. *Annu. Rev. Phys. Chem.* 67, 65–89
5. Stranks, S.D. *et al.* (2013) Electron-hole diffusion lengths exceeding 1 micrometer in an organometal trihalide perovskite absorber. *Science* 342, 341–344
6. Stoumpos, C.C. and Kanatzidis, M.G. (2015) The renaissance of halide perovskites and their evolution as emerging semiconductors. *Acc. Chem. Res.* 48, 2791–2802
7. Saparov, B. and Mitzi, D.B. (2016) Organic-inorganic perovskites: structural versatility for functional materials design. *Chem. Rev.* 116, 4558–4596
8. Tanaka, K. *et al.* (2005) Image charge effect on two-dimensional excitons in an inorganic-organic quantum-well crystal. *Phys. Rev. B* 71, 045312
9. Hong, X. *et al.* (1992) Dielectric confinement effect on excitons in lead tetraiodide-based layered semiconductors. *Phys. Rev. B Condens. Matter* 45, 6961–6964
10. Katan, C. *et al.* (2019) Quantum and dielectric confinement effects in lower-dimensional hybrid perovskite semiconductors. *Chem. Rev.* 119, 3140–3192
11. Sutherland, B.R. and Sargent, E.H. (2016) Perovskite photonic sources. *Nat. Photonics* 10, 295
12. Zhang, Y. *et al.* (2016) Synthesis, properties, and optical applications of low-dimensional perovskites. *Chem. Commun.* 52, 13637–13655
13. Mao, L. *et al.* (2019) Two-dimensional hybrid halide perovskites: principles and promises. *J. Am. Chem. Soc.* 141, 1171–1190
14. Eaton, S.W. *et al.* (2016) Lasing in robust cesium lead halide perovskite nanowires. *Proc. Natl. Acad. Sci. U. S. A.* 113, 1993–1998
15. Saouma, F.O. *et al.* (2017) Selective enhancement of optical nonlinearity in two-dimensional organic-inorganic lead iodide perovskites. *Nat. Commun.* 8, 742
16. Wang, N. *et al.* (2016) Perovskite light-emitting diodes based on solution-processed self-organized multiple quantum wells. *Nat. Photonics* 10, 699–704
17. Yuan, M. *et al.* (2016) Perovskite energy funnels for efficient light-emitting diodes. *Nat. Nanotechnol.* 11, 872
18. Li, L. *et al.* (2017) Tailored engineering of an unusual $(C_4H_9NH_3)_2(CH_3NH_3)_2Pb_3I_{10}$ two-dimensional multilayered perovskite ferroelectric for a high-performance photodetector. *Angew. Chem. Int. Ed.* 56, 12150–12154
19. Han, S. *et al.* (2018) Exploring a polar two-dimensional multi-layered hybrid perovskite of $(C_5H_{11}NH_3)_2(CH_3NH_3)Pb_2I_7$ for ultrafast-responding photodetection. *Laser Photonics Rev.* 12, 1800060
20. Gong, X. *et al.* (2018) Electron–phonon interaction in efficient perovskite blue emitters. *Nat. Mater.* 17, 550–556
21. Tsai, H. *et al.* (2016) High-efficiency two-dimensional Ruddlesden-Popper perovskite solar cells. *Nature* 536, 312–316

22. Wei, M. *et al.* (2019) Ultrafast narrowband exciton routing within layered perovskite nanoplatelets enables low-loss luminescent solar concentrators. *Nat. Energy* 4, 197–205
23. Dou, L. *et al.* (2015) Atomically thin two-dimensional organic-inorganic hybrid perovskites. *Science* 349, 1518–1521
24. Stoumpos, C.C. *et al.* (2016) Ruddlesden–Popper hybrid lead iodide perovskite 2D homologous semiconductors. *Chem. Mater.* 28, 2852–2867
25. Dohner, E.R. *et al.* (2014) Intrinsic white-light emission from layered hybrid perovskites. *J. Am. Chem. Soc.* 136, 13154–13157
26. Mao, L. *et al.* (2017) White-light emission and structural distortion in new corrugated two-dimensional lead bromide perovskites. *J. Am. Chem. Soc.* 139, 5210–5215
27. Kamminga, M.E. *et al.* (2017) The role of connectivity on electronic properties of lead iodide perovskite-derived compounds. *Inorg. Chem.* 56, 8408–8414
28. Quan, L.N. *et al.* (2016) Ligand-stabilized reduced-dimensionality perovskites. *J. Am. Chem. Soc.* 138, 2649–2655
29. Smith, I.C. *et al.* (2014) A layered hybrid perovskite solar-cell absorber with enhanced moisture stability. *Angew. Chem. Int. Ed.* 53, 11232–11235
30. Du, K-z. *et al.* (2017) Two-dimensional lead(II) halide-based hybrid perovskites templated by acene alkylamines: crystal structures, optical properties, and piezoelectricity. *Inorg. Chem.* 56, 9291–9302
31. Hu, T. *et al.* (2016) Mechanism for broadband white-light emission from two-dimensional (110) hybrid perovskites. *J. Phys. Chem. Lett.* 7, 2258–2263
32. Billing, D.G. and Lemmerer, A. (2007) Synthesis, characterization and phase transitions in the inorganic-organic layered perovskite-type hybrids $(C_nH_{2n+1}NH_3)_2PbI_4$, n = 4, 5 and 6. *Acta Crystallogr. B* 63, 735–747
33. Lemmerer, A. and Billing, D.G. (2012) Synthesis, characterization and phase transitions of the inorganic–organic layered perovskite-type hybrids $[(C_nH_{2n+1}NH_3)_2PbI_4]$, n = 7, 8, 9 and 10. *Dalton Trans.* 41, 1146–1157
34. Smith, I.C. *et al.* (2017) Between the sheets: postsynthetic transformations in hybrid perovskites. *Chem. Mater.* 29, 1868–1884
35. Passarelli, J.V. *et al.* (2018) Enhanced out-of-plane conductivity and photovoltaic performance in n = 1 layered perovskites through organic cation design. *J. Am. Chem. Soc.* 140, 7313–7323
36. Zhao, L. *et al.* (2018) Donor/acceptor charge-transfer states at two-dimensional metal halide perovskite and organic semiconductor interfaces. *ACS Energy Lett.* 3, 2708–2712
37. Ishihara, T. *et al.* (1990) Optical properties due to electronic transitions in two-dimensional semiconductors $(C_nH_{2n+1}NH_3)_2PbI_4$. *Phys. Rev. B: Condens. Matter* 42, 11099–11107
38. Calabrese, J. *et al.* (1991) Preparation and characterization of layered lead halide compounds. *J. Am. Chem. Soc.* 113, 2328–2330
39. Papavassiliou, G.C. (1997) Three- and low-dimensional inorganic semiconductors. *Prog. Solid State Chem.* 25, 125–270
40. Mitzi, D.B. (1999) Synthesis, structure, and properties of organic-inorganic perovskites and related materials. *Prog. Inorg. Chem.* 48, 1–121
41. Soe, C.M.M. *et al.* (2018) Understanding film formation morphology and orientation in high member 2D Ruddlesden–Popper perovskites for high-efficiency solar cells. *Adv. Energy Mater.* 8, 1700979
42. Grancini, G. and Nazeeruddin, M.K. (2019) Dimensional tailoring of hybrid perovskites for photovoltaics. *Nat. Rev. Mater.* 4, 4–22
43. Mao, L. *et al.* (2018) Hybrid Dion–Jacobson 2D lead iodide perovskites. *J. Am. Chem. Soc.* 140, 3775–3783
44. Soe, C.M.M. *et al.* (2017) New type of 2D perovskites with alternating cations in the interlayer space, $(C(NH_2)_3)(CH_3NH_3)_nPb_nI3_{n+1}$: structure, properties, and photovoltaic performance. *J. Am. Chem. Soc.* 139, 16297–16309
45. Lanty, G. *et al.* (2014) Room-temperature optical tunability and inhomogeneous broadening in 2D-layered organic–inorganic perovskite pseudobinary alloys. *J. Phys. Chem. Lett.* 5, 3958–3963
46. Straus, D.B. and Kagan, C.R. (2018) Electrons, excitons, and phonons in two-dimensional hybrid perovskites: connecting structural, optical, and electronic properties. *J. Phys. Chem. Lett.* 9, 1434–1447
47. Blancon, J.C. *et al.* (2018) Scaling law for excitons in 2D perovskite quantum wells. *Nat. Commun.* 9, 2254
48. Solis-Ibarra, D. *et al.* (2015) Post-synthetic halide conversion and selective halogen capture in hybrid perovskites. *Chem. Sci.* 6, 4054–4059
49. Solis-Ibarra, D. and Karunadasa, H.I. (2014) Reversible and irreversible chemisorption in nonporous-crystalline hybrids. *Angew. Chem. Int. Ed.* 53, 1039–1042
50. Smith, M.D. *et al.* (2017) Decreasing the electronic confinement in layered perovskites through intercalation. *Chem. Sci.* 8, 1960–1968
51. García-Benito, I. *et al.* (2018) Fashioning fluorous organic spacers for tunable and stable layered hybrid perovskites. *Chem. Mater.* 30, 8211–8220
52. Smith, M.D. *et al.* (2017) Structural origins of broadband emission from layered Pb–Br hybrid perovskites. *Chem. Sci.* 8, 4497–4504
53. Cortecchia, D. *et al.* (2017) Broadband emission in two-dimensional hybrid perovskites: the role of structural deformation. *J. Am. Chem. Soc.* 139, 39–42
54. Cortecchia, D. *et al.* (2017) Polaron self-localization in white-light emitting hybrid perovskites. *J. Mater. Chem. C* 5, 2771–2780
55. Yin, J. *et al.* (2017) Excitonic and polaronic properties of 2D hybrid organic–inorganic perovskites. *ACS Energy Lett.* 2, 417–423
56. Emin, D. (2012) *Polarons*, Cambridge University Press
57. Booker, E.P. *et al.* (2017) Formation of long-lived color centers for broadband visible light emission in low-dimensional layered perovskites. *J. Am. Chem. Soc.* 139, 18632–18639
58. Yangui, A. *et al.* (2015) Optical investigation of broadband white-light emission in self-assembled organic–inorganic perovskite $(C_6H_{11}NH_3)2PbBr_4$. *J. Phys. Chem. C* 119, 23638–23647
59. Cao, D.H. *et al.* (2015) 2D homologous perovskites as light-absorbing materials for solar cell applications. *J. Am. Chem. Soc.* 137, 7843–7850
60. Chen, A.Z. *et al.* (2018) Origin of vertical orientation in two-dimensional metal halide perovskites and its effect on photovoltaic performance. *Nat. Commun.* 9, 1336
61. Tsai, H. *et al.* (2018) Stable light-emitting diodes using phase-pure Ruddlesden–Popper layered perovskites. *Adv. Mater.* 30, 1704217
62. Miyata, K. *et al.* (2017) Lead halide perovskites: crystal-liquid duality, phonon glass electron crystals, and large polaron formation. *Sci. Adv.* 3, e1701469
63. Wu, X. *et al.* (2015) Excitonic many-body interactions in two-dimensional lead iodide perovskite quantum wells. *J. Phys. Chem. C* 119, 14714–14721
64. Chernikov, A. *et al.* (2015) Population inversion and giant bandgap renormalization in atomically thin WS2 layers. *Nat. Photonics* 9, 466
65. Haug, H. and Koch, S.W. (2009) *Quantum Theory of the Optical and Electronic Properties of Semiconductors*. (5th edn), World Scientific Publishing, pp. 1–469
66. Ni, L. *et al.* (2017) Real-time observation of exciton–phonon coupling dynamics in self-assembled hybrid perovskite quantum wells. *ACS Nano* 11, 10834–10843
67. Guo, P. *et al.* (2018) Cross-plane coherent acoustic phonons in two-dimensional organic-inorganic hybrid perovskites. *Nat. Commun.* 9, 2019
68. Thouin, F. *et al.* (2019) Phonon coherences reveal the polaronic character of excitons in two-dimensional lead halide perovskites. *Nat. Mater.* 18, 349–356
69. Straus, D.B. *et al.* (2016) Direct observation of electron–phonon coupling and slow vibrational relaxation in organic–inorganic hybrid perovskites. *J. Am. Chem. Soc.* 138, 13798–13801
70. Skolnick, M.S. and Bimberg, D. (1978) Angular-dependent magnetoluminescence study of the layer compound 2H-PbI_2. *Phys. Rev. B* 18, 7080–7088

71. Neutzner, S. *et al.* (2018) Exciton-polaron spectral structures in two-dimensional hybrid lead-halide perovskites. *Phys. Rev. Mater.* 2, 064605
72. Nishida, J. *et al.* (2018) Dynamically disordered lattice in a layered Pb-I-SCN perovskite thin film probed by two-dimensional infrared spectroscopy. *J. Am. Chem. Soc.* 140, 9882–9890
73. Thouin, F. *et al.* (2018) Stable biexcitons in two-dimensional metal-halide perovskites with strong dynamic lattice disorder. *Phys. Rev. Lett.* 2, 034001
74. Zhu, X.Y. and Podzorov, V. (2015) Charge carriers in hybrid organic-inorganic lead halide perovskites might be protected as large polarons. *J. Phys. Chem. Lett.* 6, 4758–4761
75. Zhu, H. *et al.* (2016) Screening in crystalline liquids protects energetic carriers in hybrid perovskites. *Science* 353, 1409–1413
76. Yaffe, O. *et al.* (2017) Local polar fluctuations in lead halide perovskite crystals. *Phys. Rev. Lett.* 118, 136001
77. Ema, K. *et al.* (2008) Nearly perfect triplet-triplet energy transfer from Wannier excitons to naphthalene in organic-inorganic hybrid quantum-well materials. *Phys. Rev. Lett.* 100, 257401
78. Ema, K. *et al.* (2006) Huge exchange energy and fine structure of excitons in an organic-inorganic quantum well material. *Phys. Rev. B* 73, 241310
79. Tanaka, K. *et al.* (2002) Two-dimensional Wannier excitons in a layered-perovskite-type crystal $(C_6H_{13}NH_3)2PbI_4$. *Solid State Commun.* 122, 249–252
80. Kataoka, T. *et al.* (1993) Magneto-optical study on the excitonic spectrum of $(C_6H_{13}NH_3)2PbI_4$. *Phys. B Condens. Matter* 184, 132–136
81. Even, J. *et al.* (2015) Solid-state physics perspective on hybrid perovskite semiconductors. *J. Phys. Chem. C* 119, 10161–10177
82. Kepenekian, M. *et al.* (2015) Rashba and Dresselhaus effects in hybrid organic–inorganic perovskites: from basics to devices. *ACS Nano* 9, 11557–11567
83. Isarov, M. *et al.* (2017) Rashba effect in a single colloidal $CsPbBr_3$ perovskite nanocrystal detected by magneto-optical measurements. *Nano Lett.* 17, 5020–5026
84. Zhai, Y. *et al.* (2017) Giant Rashba splitting in 2D organic-inorganic halide perovskites measured by transient spectroscopies. *Sci. Adv.* 3, e1700704
85. Yin, J. *et al.* (2018) Layer-dependent Rashba band splitting in 2D hybrid perovskites. *Chem. Mater.* 30, 8538–8545
86. Zhang, X. *et al.* (2018) First-principles analysis of radiative recombination in lead-halide perovskites. *ACS Energy Lett.* 3, 2329–2334
87. Marronnier, A. *et al.* (2018) Influence of disorder and an harmonic fluctuations on the dynamical Rashba effect in purely inorganic lead-halide perovskites. *J. Phys. Chem. C* 123, 291–298
88. Kitazawa, N. *et al.* (2012) Temperature-dependent time-resolved photoluminescence of $(C_6H_5C_2H_4NH_3)_2PbX_4$ (X=Br and I). *Mater. Chem. Phys.* 134, 875–880
89. Younts, R. *et al.* (2017) Efficient generation of long-lived triplet excitons in 2D hybrid perovskite. *Adv. Mater.* 29, 1604278
90. Kitazawa, N. *et al.* (2010) Excitons in organic–inorganic hybrid compounds $(C_nH_{2n+1}NH_3)_2PbBr_4$ (n=4, 5, 7 and 12). *Thin Solid Films* 518, 3199–3203
91. Mitzi, D.B. *et al.* (2001) Organic-inorganic electronics. *IBM J. Res. Dev.* 45, 29–45
92. Williams, O.F. *et al.* (2018) Energy transfer mechanisms in layered 2D perovskites. *J. Chem. Phys.* 148, 134706
93. Zheng, K. *et al.* (2018) Inter-phase charge and energy transfer in Ruddlesden–Popper 2D perovskites: critical role of the spacing cations. *J. Mater. Chem. A* 6, 6244–6250
94. Liu, J. *et al.* (2017) Observation of internal photoinduced electron and hole separation in hybrid two-dimensional perovskite films. *J. Am. Chem. Soc.* 139, 1432–1435
95. Gélvez-Rueda, M.C. *et al.* (2017) Interconversion between free charges and bound excitons in 2D hybrid lead halide perovskites. *J. Phys. Chem. C* 121, 26566–26574
96. Blancon, J.C. *et al.* (2017) Extremely efficient internal exciton dissociation through edge states in layered 2D perovskites. *Science* 355, 1288–1292
97. Leyden, M.R. *et al.* (2018) Amplified spontaneous emission in phenylethylammonium methylammonium lead iodide quasi-2D perovskites. *Phys. Chem. Chem. Phys.* 20, 15030–15036
98. Zhang, S. *et al.* (2009) Synthesis and optical properties of novel organic–inorganic hybrid nanolayer structure semiconductors. *Acta Mater.* 57, 3301–3309
99. Kamminga, M.E. *et al.* (2016) Confinement effects in low-dimensional lead iodide perovskite hybrids. *Chem. Mater.* 28, 4554–4562
100. Dohner, E.R. *et al.* (2014) Self-assembly of broadband white-light emitters. *J. Am. Chem. Soc.* 136, 1718–1721
101. Guo, P. *et al.* (2018) Hyperbolic dispersion arising from anisotropic excitons in two-dimensional perovskites. *Phys. Rev. Lett.* 121, 127401